Absence of stable intermediates on the folding pathway of barnase

Jiro Takei, Rui-Ai Chu, and Yawen Bai*

Laboratory of Biochemistry, National Cancer Institute, National Institutes of Health, Building 37, Room 4A-01, Bethesda, MD 20892

Edited by Robert L. Baldwin, Stanford University Medical Center, Stanford, CA, and approved July 14, 2000 (received for review June 8, 2000)

Barnase is one of the few protein models that has been studied extensively for protein folding. Previous studies led to the conclusion that barnase folds through a very stable submillisecond intermediate (≈3 kcal/mol). The structure of this intermediate was characterized intensively by using a protein engineering approach. This intermediate has now been reexamined with three direct and independent methods. (*i*) Hydrogen exchange experiments show very small protection factors (≈2) for the putative intermediate, indicating a stability of ≈0.0 kcal/mol. (*ii*) Denaturant-dependent unfolding of the putative intermediate is noncooperative and indicates a stability less than 0.0 kcal/mol. (*iii*) The logarithm of the unfolding rate constant of native barnase vs. denaturant concentrations is not linear. Together with the measured rate ("*I*" to *N*), this nonlinear behavior accounts for almost all of the protein stability, leaving only about 0.3 kcal/mol that could be attributed to the rapidly formed intermediate. Other observations previously interpreted to support the presence of an intermediate are now known to have alternative explanations. These results cast doubts on the previous conclusions on the nature of the early folding state in barnase and therefore should have important implications in understanding the early folding events of barnase and other proteins in general.

Barnase folds in multiple kinetic phases at pH 6.3 and 25°C (1). A submillisecond burst phase is observed (2). Approximately 80% of the molecules then fold in a fast single exponential phase with a folding rate constant k_f of ≈13 s^{-1}. The other 20% folds slowly because of *cis–trans* isomerization of prolines (1). In the earlier studies of the folding pathway of barnase, Fersht and coworkers (1) concluded that the major kinetic folding phase represented the folding from a stable submillisecond intermediate to the native state. This conclusion was based on the following experimental results. (*i*) There was a loss of CD signal within the submillisecond burst phase (2), consistent with a fast intermediate. (*ii*) The log k_f (folding rate constant) as a function of denaturant concentrations is not linear (1), as illustrated in the chevron plot in Fig. 1, consistent with an on-pathway intermediate. (*iii*) An H/D pulse-labeling experiment revealed strong protections for some amide protons within 6 ms, suggesting a very stable intermediate (3). (*iv*) The stability for the intermediate was calculated to be 3.2 kcal/mol, taken as the difference between the equilibrium unfolding free energy for native barnase (ΔG_{NU}) and the free energy for the major folding phase, ΔG_u^{app}, calculated as $-RT\ln(k_u/k_f)$ (1). Here, k_u is the unfolding rate constant extrapolated from the right limb of the chevron plot assuming a linear relationship between log k_u and denaturant concentrations (see illustrations in Fig. 1).

Recent progress in protein-folding studies questioned these conclusions. (*i*) The burst phase signal lost within submilliseconds may simply represent the conformational readjustment of the unfolded state to lower denaturant concentrations as suggested for cytochrome *c* and ribonuclease A (4, 5). (*ii*) Alternative interpretations such as movement of the transition state ensemble can explain curved chevron plots, as proposed for Arc repressor (6) and U1A (7). (*iii*) A more recent hydrogen-exchange (HX) pulse-labeling experiment could not reproduce the earlier barnase results and failed to detect any stable intermediate (8). (*iv*) A native-state HX experiment also failed to reveal the postulated intermediate (9). (*v*) The correct extrapolation of log k_u may curve downward at low denaturant concentrations, as has been shown for several proteins including Arc repressor (6), U1A (7), protein L (10), and CI2 (11). This nonlinear behavior would increase the calculated ΔG_u^{app} for the major folding phase and decrease the calculated stability left over for the putative intermediate. These alternative interpretations and new experimental results suggest that the earlier conclusion needs to be reexamined by using more direct methods. Such a reexamination is important, because barnase has been taken as a classical illustration of how proteins fold, and its intermediate has been characterized intensively with a protein-engineering approach (12). In particular, a definite conclusion on the postulated intermediate of barnase will help to understand the ability and limitations of both the protein-engineering and the native-state HX approaches (1, 13). This article reports a reexamination of these issues.

Materials and Methods

Materials. Proteins and buffer solutions were prepared as described (8).

Folding and HX Competition Experiments. The folding-HX competition experiments (14) were performed with a Biologic QFM-4 (Grenoble, France; dead time ≈1 ms). Folding of denatured barnase (≈10 mg/ml) in 3.20 M deuterated GdmCl solution (pD 6.3, 10 mM Mes/D_2O) was initiated by a 20-fold dilution with a buffer solution (pH 6.3, 50 mM Mes/H_2O) at 25°C. Reactions were allowed to proceed for several minutes before pH was adjusted to 5.0 with 0.5 M HOAc. Solutions (50 ml) were concentrated, and buffer was exchanged with a 10% (vol/vol) D_2O and 10 mM NaOAc solution with Amicon cells. The same experiment was performed at pH 7.23 (0.2 M K_2HPO_4/0.1 M Na_2SO_4). The ^1H–^{15}N heteronuclear sequential quantum correlation NMR spectra were collected on a Bruker AMX 500 spectrometer (Billerica, MA) and processed with FELIX (version 97, Biosym Technologies, San Diego). Peak intensities were used to measure the proton occupancies with amide protons Q104, R110, and W94 (4NH) averaged as internal references. Calculations of exchange rate constants, k_{ex}, and protection factors ($P_f = k_{int}/k_{ex}$) used Eq. **5** with 8 s^{-1} for k_f and intrinsic exchange rate constant, k_{int}, based on peptide models (15).

Kinetic and Equilibrium CD and Fluorescence. Stopped-flow CD experiments were performed with the Biologic SFM4. Up to 30 kinetic traces with a 1.0-cm path-length observation cell were averaged for each data point. Kinetic runs were initiated by mixing denatured barnase (pH 1.6 or 9.4 M urea) with folding

This paper was submitted directly (Track II) to the PNAS office.

Abbreviations: GdmCl, guanidinium chloride; HX, hydrogen exchange.

*To whom reprint requests should be addressed. E-mail: yawen@helix.nih.gov.

The publication costs of this article were defrayed in part by page charge payment. This article must therefore be hereby marked "*advertisement*" in accordance with 18 U.S.C. §1734 solely to indicate this fact.

Article published online before print: *Proc. Natl. Acad. Sci. USA*, 10.1073/pnas.190265797. Article and publication date are at www.pnas.org/cgi/doi/10.1073/pnas.190265797

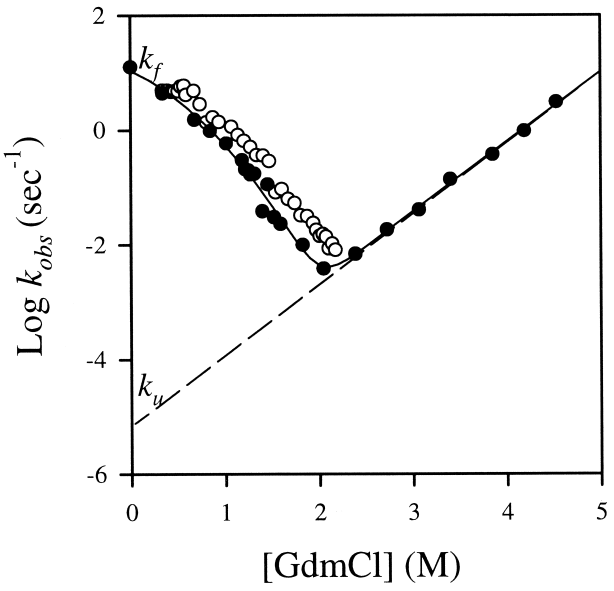

Fig. 1. Chevron curves of wild-type barnase at 25°C and pH 6.3 (solid circles) and pH 7.23 in the presence of 0.1 M Na_2SO_4 (open circles). The solid curve is the best fit of the observed rate constants to a three-state model with Eqs. **1–3**. It yields the following values: $K_{IU} = 0.009$; $m_{IU} = 4.05\ M^{-1}$; $k_{IN} = 11.9\ s^{-1}$; $m_{IN} = 2.63\ M^{-1}$; $k_{NI} = 8.6 \times 10^{-6}\ s^{-1}$; $m_{NI} = 2.80\ M^{-1}$; m_{NU} (sum of m_{IU}, m_{IN}, and m_{NI}) = 9.49 M^{-1}; and $m_{IU}/m_{NU} = 0.43$. The dashed line illustrates the linear extrapolation of unfolding rate constant log k_u. It should be noted that the k_u in water, obtained with guanidinium chloride (GdmCl) and linear extrapolation, is 10 times smaller than the value obtained with urea (1).

buffer (pH 6.3, 50 mM Mes) with a final protein concentration of 14.6 μM (extinction coefficient 25,900 $M^{-1}\cdot cm^{-1}$ at 280 nm). Stopped-flow fluorescence was performed similarly at $\approx$3 μM protein concentration.

Three-State Chevron Curve Fitting. Chevron curves were fitted according to Eqs. **1–3** assuming U and I are in rapid equilibration, following Raschke and Marqusee (16).

$$U \underset{k_{IU}}{\overset{k_{UI}}{\rightleftharpoons}} I \underset{k_{NI}}{\overset{k_{IN}}{\rightleftharpoons}} N \qquad [1]$$

and

$$k_{obs} = [1/(1 + K_{IU})]k_{IN} + k_{NI}\,. \qquad [2]$$

$$k_{obs}([Den]) = \{1/[1 + K_{IU}{}^{H_2O}e^{(m_{IU}[Den])}]\}k_{IN}{}^{H_2O}e^{(m\ddagger_{IN}[Den])} + k_{NI}{}^{H_2O}e^{(m\ddagger_{NI}[Den])}, \qquad [3]$$

where $K_{IU}{}^{H2O}$ is the unfolding equilibrium constant of the intermediate in water; $k_{IN}{}^{H2O}$ and $k_{NI}{}^{H2O}$ are the values of the corresponding microscopic rate constants in the absence of denaturant; and $m\ddagger_{IN}$ and $m\ddagger_{NI}$ are the coefficients for the denaturant dependence of the microscopic rate constants.

Intermediate Melting Curve Fitting. The unfolding equilibrium constant of the intermediate K_{IU} was obtained by assuming a linear dependence of log K_{IU} on urea concentration and fitting the standard Santoro–Bolen equation (17) with floating parameters for baselines. The complete equation used for the fitting is

$$I([Den]) = \{\alpha_I[Den] + \beta_I + [K_{IU}{}^{H_2O}e^{(m_{IU}[Den])}]\cdot (\alpha_U[Den] + \beta_U)\}/\{1 + K_{IU}{}^{H_2O}e^{(m_{IU}[Den])}\}\,, \qquad [4]$$

where I is the value of the CD signal; $K_{IU}{}^{H2O}$ is the unfolding equilibrium constant of the intermediate in water; α_I, β_I, α_U, and β_U are the parameters of the baselines for the intermediate (I) and unfolded (U) states, respectively; and m_{IU} is the coefficient for the denaturant dependence of the ln K_{IU}. All curve fittings were carried out with SIGMAPLOT (SPSS, Chicago).

Results

Principles for Measurement of the Stability of the Early Folding State from HX Protection Factors. The stability of the early folding state of barnase can be determined based on the protection factors of the slowly exchanging amide protons, because 13 amide protons of barnase exchange with solvent protons only through global unfolding (9, 18). Fersht and coworkers have shown: (*i*) the averaged ΔG_{HX} values for these protons are in excellent agreement with the ΔG_{NU} values measured by differential scanning calorimetry (18), where ΔG_{HX} is defined as $-RT\ln(k_{ex}/k_{int})$; (*ii*) the changes of the global unfolding free energy ($\Delta\Delta G_{NU}$) are the same as $\Delta\Delta G_{HX}$ between wild-type barnase and the mutants for the 13 amide protons (18); and (*iii*) the HX rates of these amide protons are accelerated at very low concentrations of GdmCl (9). These results require that no exchange occurs for the 13 amide protons through any structural fluctuations in N or any intermediate state, other than the fully unfolded state (9, 18). Thus, the P_f measured after the intermediate is formed for these protons should reflect the stability (I to U) of the proposed intermediate state with the relationship between $\Delta G_{IU} = -RT\ln[1/(P_f - 1)]$ (19). For example, if the proposed folding intermediate of barnase has a stability of $\approx$3.0 kcal/mol as suggested previously (1), all of the 13 amide protons would be protected by a factor of >100 in the intermediate.

The Protection Factors of the Amide Protons in the Early Folding State of Barnase Measured by Competition HX. To explore the stability of the proposed intermediate, we directly measured HX rate constants of amide protons in the early folding state of barnase by using the competition HX method (14). In this experiment, unfolded barnase in D_2O and denaturant was diluted with H_2O solution to initiate folding and HX reactions. Folding was allowed to proceed for several minutes to completion. In the native state, many amide protons are protected from exchange for weeks, which allows the fractions of the ^1H [$P_{occ}(H)$] exchanged during the HX-folding process to be measured by using NMR from folded barnase. Because the stability of barnase decreases significantly, and the chevron plots became less curved at pHs above 7.5 (20), we performed competition experiments at two different pHs: 6.3 and 7.23. These experiments used the following relationship among k_{ex}, k_f, and $P_{occ}(H)$ for barnase when the competition proceeded until native proteins were formed completely (14):

$$P_{occ}(H) = 0.8\ k_{ex}/(k_{ex} + k_f) + 0.2. \qquad [5]$$

The factors 0.8 and 0.2 represent the fraction of the *trans* (fast folding) and *cis* (slow folding) proline isomers in the unfolded state, as determined by Matouschek *et al.* (1, 12). If one measures $P_{occ}(H)$ and k_f, then k_{ex} can be calculated (Eq. **5**), and P_f can be obtained ($P_f = k_{int}/k_{ex}$). At pH 6.3 and 25°C, 3 (K19, S50, and S91) of the 13 amide protons have large k_{int} (13, 10, and 9 s^{-1}, respectively), which is comparable to the k_f (8 s^{-1}) of barnase at 0.16 M GdmCl. Therefore, the k_{ex} of these protons can be measured accurately in the competition experiment. The P_f values for the three amide protons K19, S50, and S91 were 1.7, 1.5, and 1.1, respectively. These numbers are typical of amide protons in unfolded polypeptide chains (15).

The same competition experiment was performed at a slightly higher pH (7.23) in the presence of 0.1 M Na_2SO_4. The stabilizing salt ensures that the proposed intermediate, if it exists,

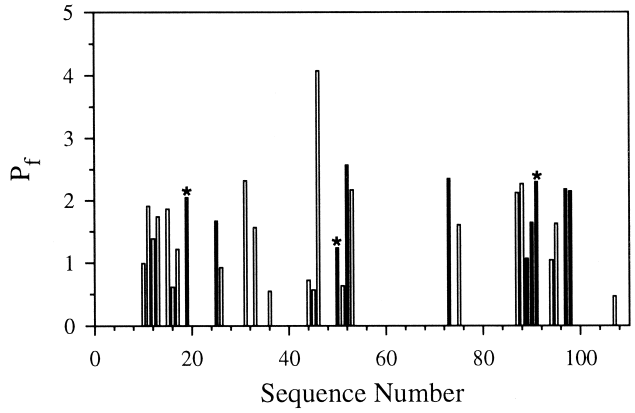

Fig. 2. HX protection factors in the early folding state. The filled bars are the P_f values of the 13 amide protons. The asterisks indicate the averaged P_f measured at both pH 6.3 and 7.23. Others in open bars are at pH 7.23.

should be more stable. This further stabilization is illustrated by the right shift of the folding limb of the chevron plot (Fig. 1). At pH 7.23, the HX protection of many additional amide protons can be measured directly. All of the amide protons that could be identified and resolved in the two-dimensional ^1H–^{15}N correlation spectrum (21) have P_f values between 0.5 and 2.5, except for one close to 4.5 (Fig. 2). Similar results were obtained in the presence of 0.1 M Na_2SO_4 at 0.0 and 0.36 M urea and at higher concentrations of Na_2SO_4 (up to 0.4 M, unpublished results). Importantly, the 13 amide protons are not protected more than others. The average P_f for the slowly exchanging amide protons is about 2. This value leads to a K_{IU} of 1.0 and a ΔG_{IU} value of $\approx$0.0 kcal/mol.

Noncooperative Melting of the Early Folding State by Urea. The stability of the early folding state of barnase was also explored directly by using CD and fluorescence. For barnase, the strongest CD signal in the far UV region at wavelength of 230 nm provides the information of secondary structures (2). The fluorescence signal, excited at 280 nm and collected above 310 nm, reflects the environment of the tryptophan residues in barnase. We measured the amplitude of these signals for the early folding state from the kinetic traces for barnase folding at 10 ms as a function of urea concentration by using a stopped-flow apparatus. By 10 ms, all of the burst phase intermediate is formed, and almost none has gone forward to N ($k_f \approx 13\ s^{-1}$). The urea dependence of the amplitude therefore reflects how the proposed intermediate of barnase unfolds by denaturant at pH 6.3 and 25°C. Two examples of the kinetic traces are shown in Fig. 3 *A* and *B*. The

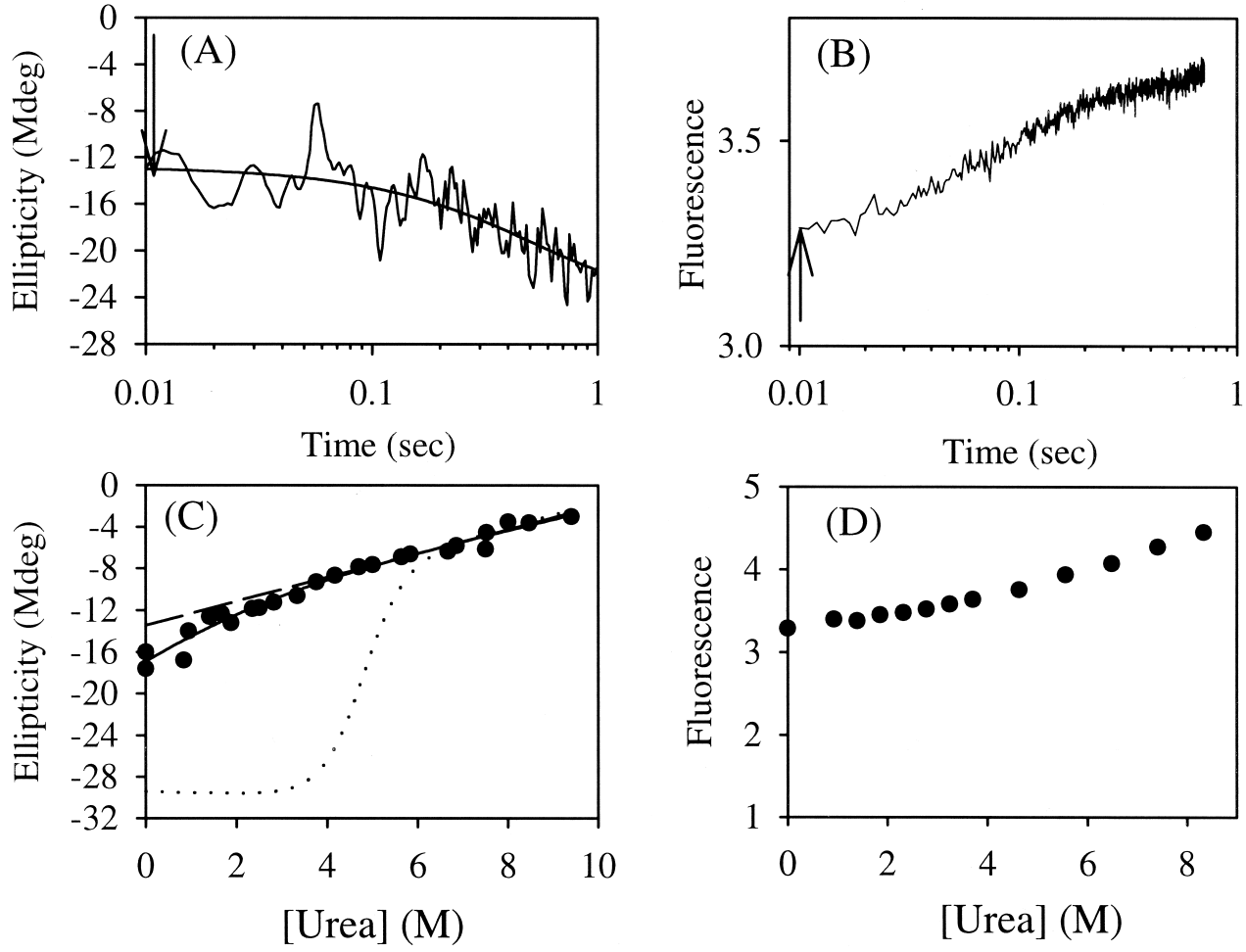

Fig. 3. Noncooperative unfolding of the postulated intermediate. Kinetic traces generated by the stopped-flow CD at 0.94 M urea (*A*) and fluorescence in water (*B*) at pH 6.3 and 25°C. The values at 10 ms of folding as indicated by the arrows at different urea concentrations were plotted in *C* (solid circles) and *D* (solid circles). The global unfolding of barnase is shown with the dotted line. The curved solid line is the fitting curve with a two-state model with parameters for both pretransition and posttransition baselines (see *Materials and Methods*). The dashed line represents the posttransition baseline. Mdeg, millidegree.

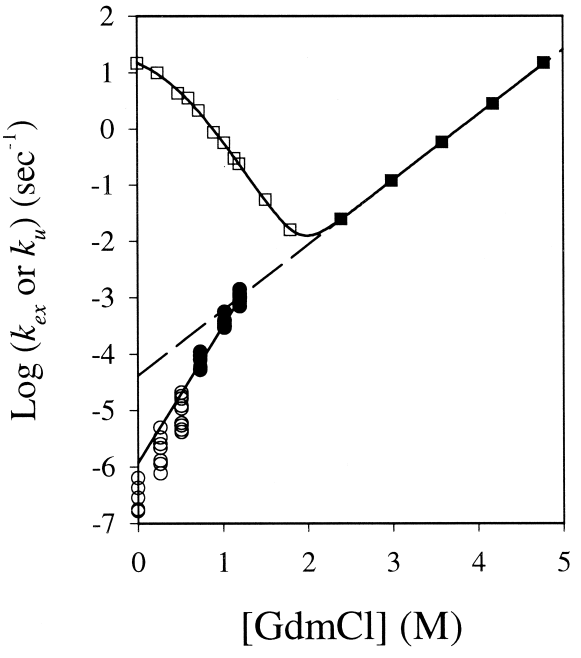

Fig. 4. Downward deviation of the log k_u at 30°C and pD 6.8 (pD_{read} + 0.4) in D_2O. The open and filled squares are rate constants measured by using stopped-flow fluorescence under the conditions used in the native-state HX experiments (9). The open and filled circles represent the HX rate constants of the slowly exchanging amide protons measured at GdmCl concentrations from 0.0 to 0.51 M and from 0.73 M to 1.20 M, respectively (9). The convergence of the exchange rate constants of the 13 amide protons at above 0.51 M GdmCl is indicative of EX1 exchange mechanism. The solid straight line represents the linear fitting of the filled circles with a slope of 2.425 and an intercept of −5.924. The dashed line is the linear fitting to the log k_u at higher GdmCl concentrations.

values measured (shown in Fig. 3 *C* and *D)* did not show a sigmoid type of cooperative transition, although small deviations from linearity are observable. These results are very similar to the behavior of nonfolding cytochrome *c* fragments (4) and the unfolded, disulfide-broken state of ribonuclease A (5), suggesting that the early folding state of barnase may not be a discrete folding intermediate. The change in CD and fluorescence signals within submilliseconds may simply represent the conformational readjustment of the unfolded state under different solvent conditions. When the CD values were fitted to a two-state cooperative unfolding model with floating parameters for both pretransition and posttransition baselines (see Eq. **4**), we obtained a value of 2.6 for K_{IU} (= $[U]/[I]$), indicating that the putative intermediate state is even less stable than the unfolded state by 0.6 kcal/mol. This value is expected from an incomplete transition curve (Fig. 3*C*).

Direct Observation of Nonlinear Behavior of log k_u vs. GdmCl Concentrations. If the postulated intermediate is not as stable as proposed previously or does not exist, one expects that ΔG_{NU}, measured by equilibrium melting, will be equal to $-RT\ln(k_u/k_f)$. This expectation is consistent with measured rates (Fig. 1) only if log k_u is downward curved at lower denaturant concentrations. A reanalysis of the previous native-state HX results by Clarke and Fersht (9) indicated that this nonlinear behavior is indeed the case (Fig. 4).

Because the 13 slowly exchanging amide protons can exchange only through global unfolding, their exchange process (in D_2O) can be written as in reaction scheme (6) with the intermediate state and the unfolded state included in the effective unfolded

Table 1. ΔG_{HX} values for the slowly exchanging amide protons at 0.0 M GdmCl, 30°C, pD 6.8 (pD_{read} + 0.4) in D_2O

Residue number	k_{ex}, s^{-1}*	k_{int}, s^{-1}†	ΔG_{HX}, kcal/mol
19	2.83×10^{-7}	7.3	10.3
50	4.27×10^{-7}	8.5	10.1
52	1.63×10^{-7}	3.0	10.1
98	1.77×10^{-7}	2.8	10.0
Average			10.1

It should be noted that Clarke and Fersht (9) obtained higher ΔG_{HX} values. Obviously, they used different k_{int}. An independent check of the k_{int} values can be made easily by using the program on the web site http://dino.fold.fccc.edu:8080/sphere.html.

*Values of k_{ex} are from Clarke and Fersht (9).

†Values of k_{int} are from Bai *et al.* (15).

state U^{eff} ($U + I$). This treatment is because proton signals were monitored only in the native state to measure the HX rates (see detailed discussions in ref. 22 about HX process for a three-state model).

$$N(H) \underset{k_f^{eff}}{\overset{k_u}{\rightleftharpoons}} U^{eff}(H) \xrightarrow{k_{int}^{eff}} U^{eff}(D). \qquad [6]$$

Here, k_{int}^{eff} and k_f^{eff} are the effective exchange rate constant and the effective rate constant of generating the native state, respectively. The measured exchange rate constant k_{ex} can be written as $k_{ex} = k_u\, k_{int}^{eff}/(k_f^{eff} + k_{int}^{eff})$. It follows that $k_{ex} = k_u$ if $k_{int}^{eff} \gg k_f^{eff}$ (EX1 mechanism) and $k_{ex} = k_u/k_f^{eff} = K_u$ if $k_{int}^{eff} \ll= k_f^{eff}$ (EX2 mechanism; see discussions in ref. 22). Simply stated, equilibrium HX experiments provide a means to measure the unfolding rate constant k_u when HX occurs through EX1 mechanism and the global equilibrium unfolding constant K_u when HX occurs through an EX2 mechanism.

In the native-state HX experiments on barnase at pD 6.8 (pD_{read} + 0.4) and 30°C, it was demonstrated that the 13 slowly exchanging amide protons exchanged with solvent protons by an EX2 mechanism at 0.0 M GdmCl and by an EX1 mechanism at above 0.51 M GdmCl (9). These conclusions were based on the following findings. (*i*) The HX rate constants of these amide protons were sensitive to pH changes at 0.0 M GdmCl but became independent of pH at GdmCl concentrations higher than 0.51 M GdmCl. (*ii*) The HX rate constants were different for different amide protons at 0.0 M GdmCl, but they converged to the same value at above 0.51 M GdmCl (see Fig. 4). Therefore, at 0.0 M GdmCl, the ΔG_{HX} for these amide protons should represent the global unfolding free energy ΔG_{NU}. Above 0.51 M GdmCl, the measured k_{ex} should represent k_u.

Table 1 lists the ΔG_{HX} values for the four slowly exchanging amide protons measured at 0.0 M GdmCl. The averaged value is 10.1 kcal/mol. Fig. 4 shows that the log k_u at 0.0 M GdmCl extrapolated from the HX rate constants measured under EX1 mechanism (above 0.7 M GdmCl) is −5.92. Because the directly measured folding rate constant k_f is 14.7 s^{-1}, the ΔG_u^{app} $[-RT\ln(k_u/k_f)]$ for barnase at 0.0 M GdmCl is calculated to be 9.8 kcal/mol. This number is only 0.3 kcal/mol smaller than the value 10.1 kcal/mol of the averaged ΔG_{HX} for the slowly exchanging amide protons (Table 1).

If a linear extrapolation is used to obtain a log k_u in D_2O from the unfolding values of the right limb of the chevron plot (Fig. 4) as done by Matouschek *et al.* (1), the value of log k_u is −4.3. This value leads to a ΔG_u^{app} of 7.6 kcal/mol, which is 2.5 kcal/mol less than the global unfolding free energy 10.1 kcal/mol. The missing stability was postulated by Matouschek *et al.* (1) to represent the stability of the early intermediate. However, the

BIOPHYSICS

Table 2. Stability of the proposed intermediate of wild-type barnase measured by different methods in kcal/mol at pH 6.3 and 25°C

	Direct methods			
	Urea melting†	Competition HX‡	Native-state HX§	Indirect methods*
ΔG_{IU}	−0.6	~0.0	0.3	2.7 to 3.2

*Values are 2.8 kcal/mol from Dalby *et al.* (24), 2.7 kcal/mol from the chevron plot fitting that used a three-state model with fixed intermediate and transition state (see *Materials and Methods* and Fig. 1), and 3.2 kcal/mol from Matouschek *et al.* (1).

†The value was obtained by fitting the CD signals (Fig. 3*C*) to a two-state model with floating parameters for both pretransition and posttransition baselines (Eq. **4**). If K_{IU} is fixed with a value of 0.25 (ΔG_{IU} = 0.8 kcal/mol), the fitting yields an m_{IU} value that is 60% of the m_{NU} value for global unfolding (20). This value is significantly larger than the 43% value obtained from the chevron curve fitting (see Fig. 1), indicating that the ΔG_{IU} is unlikely larger than 0.8 kcal/mol.

‡This value was obtained assuming an average protection factor of 2 (Fig. 2). Simulation studies that use Eq. **5** show that a ±10% error in $P_{occ}(H)$ measurement may contribute an error less than a factor of 2 in P_f, which may contribute an uncertainty in ΔG_{IU} by ~0.4 kcal/mol.

§The value was calculated from $\Delta G_u^{app} - \Delta G_{HX}$ (see text) based on the HX data of Clarke and Fersht (9). Possible uncertainties in k_{int} by a factor of 2 may contribute another error in free energy by 0.4 kcal/mol. Thus, the ΔG_{IU}s determined from both HX experiments are unlikely larger than 0.8 kcal/mol.

directly measured nonlinear log k_u shown in Fig. 4 explains the missing stability and leaves only 0.3 kcal/mol for the postulated intermediate.

Matouschek *et al.* (1) initially used an unstable mutant (L14A) to obtain log k_u values down to 0.5 M urea at pH 3.0 to justify the linear extrapolation. A linear behavior was observed in the range between 0.5 M and 3.5 M urea for this mutant. However, the slope shown from this linear fitting was clearly larger than that obtained between 3.7 M and 4.7 M urea at pH 6.3 (see figure 2 in ref. 1), consistent with a downsloping behavior. Later reexaminations of log k_u at high urea concentrations revealed some nonlinear behavior (23). In a more recent attempt, Dalby *et al.* (24) measured log k_u in a wider range of urea concentrations by extrapolating k_u values at higher temperatures to 25°C by using the Eyring equation. The same nonlinear behavior of log k_u was confirmed, but they were unable to explore the important region below 2 M urea concentrations. The native-state experiment by Clarke and Fersht (9) that entered the EX1 region now provides unfolding rates at low denaturant that clearly demonstrates the down-curving nature of the chevron unfolding limb at low urea and allows a more accurate extrapolation of k_u to zero denaturant, as shown in Fig. 4.

The stability of the postulated intermediate measured by different methods and the possible errors estimated are summarized in Table 2.

Discussion

Taken together, (*i*) the directly measured small HX protection factors, (*ii*) the noncooperative unfolding behavior of the putative early folding state, and (*iii*) the downward shifted unfolding rate constants at very low GdmCl concentrations all argue that a stable folding intermediate with a stability of ≈3 kcal/mol does not exist on the folding pathway of wild-type barnase. The proposed intermediate, if it exists, is unlikely to be more stable than the unfolded state by 0.8 kcal/mol (see footnotes in Table 2 for error estimation).

Uncertainties in the Earlier Characterization of the Intermediate of Barnase. Matouschek *et al.* (1, 12) used the protein engineering approach to determine side-chain interactions in the proposed intermediate state of barnase. This approach measures the changes of the unfolding free energy of the intermediate ($\Delta\Delta G_{IU}$) and the global unfolding free energy ($\Delta\Delta G_{NU}$) between the wild-type protein and mutants. A ϕ_I value, defined as $\Delta\Delta G_{IU}/\Delta\Delta G_{NU}$, was used to indicate the extent of the interactions between the residue that is mutated and other residues in the intermediate. If the ϕ_I value is 1.0, it suggests that the mutated residues interact with other residues in the intermediate state as strongly as in the native state. If the ϕ_I value is zero, then the interactions are as weak as in the unfolded state. A fractional ϕ_I value represents partial interactions. Because the stability of the intermediate state of wild-type barnase is less than 0.8 kcal/mol, the experimentally measured $\Delta\Delta G_{IU}$ for any mutant should not exceed this value. Thus, it provides a criterion to test the accuracy of the earlier measurements. A large number (more than 40%) of $\Delta\Delta G_{IU}$ values measured in the earlier studies by Matouschek *et al.* (12) were larger than 0.8 kcal/mol (see table 2 in ref. 12). Some of them were even larger than 2 kcal/mol. These large values suggest that there are large uncertainties in the $\Delta\Delta G_{IU}$ and ϕ_I values and in the structure of the intermediate characterized based on them. The large $\Delta\Delta G_{IU}$ values obtained by Matouschek *et al.* (1, 12) seem to result from the assumption that the measured log k_u vs. denaturant concentration, which must be extrapolated to zero denaturant, has similar linear behavior for both wild-type and mutant proteins. That is, the computed ϕ_I values incorporate the same (apparently incorrect) assumption that leads to an estimated 3 kcal/mol in stability for the supposed intermediate.

Possible Interpretations for the Curved Chevron Plot of Barnase. The significant curvature in the folding limb of the chevron plot of barnase was concluded to be due to the population of a stable intermediate by Matouschek *et al.* (1). This interpretation, however, is questionable and contrary to the experimental results presented in this article. Two alternative models have been proposed to account for the curvature in chevron plots. (*i*) Movement of the transition state ensemble as a function of denaturant alone may be responsible for the curved chevron plot. This model was suggested by Otzen *et al.* (7) and was used to explain the curved chevron plot of U1A. The curved log k_u shown in Fig. 4 seems to be consistent with this model. Movement of the transition state ensemble toward the unfolded state as protein stability increases is also expected by the Hammond postulate and was observed from earlier mutation studies on barnase (25, 26). (*ii*) The early folding state of barnase may be an ensemble of differently collapsed unfolded states. A redistribution of this ensemble as a function of denaturant concentrations may be responsible for the curvature in the chevron plot of barnase. This model was used to explain the curved chevron plots of several proteins by Parker and Marqusee (27). A combination of *i* and *ii* is also possible.

Native-State HX and Protein Engineering Approaches. Clarke *et al.* (28) questioned the usefulness of the native-state HX approach as an analytical tool to study folding pathways of proteins. They concluded that the native-state HX approach was not a reliable approach, because it was not able to identify the very stable intermediate of barnase that has been studied fully by the protein-engineering approach and the H/D pulse-labeling methods. Previously, we found that the H/D pulse-labeling experiment by Bycroft *et al.* (3) could not be reproduced, and our recent H/D pulse-labeling experiment did not detect any stable intermediate (8). The experimental results presented herein, including (*i*) the small HX protection factors, (*ii*) the noncooperative melting of the early folding state by urea, and (*iii*) the downward curved log k_u, are all consistent

with the native-state HX results, i.e., no stable intermediate seems to exist.

To conclude, the initial burst phase folding of barnase seems to reach the ensemble of forms with some characteristics that one may call the unfolded state under the conditions of the folding experiment (4, 5). Whether particular interactions or structures exist in this ensemble that help to predetermine the folding pathways remains to be seen (29). We show that any such interactions provide no net favorable free energy to the overall ensemble.

We thank Drs. S. Walter Englander, Tobin R. Sosnick, Hue Sun Chan, and Werner Klee for critical reading the paper and helpful suggestions, Dr. Joeseph J. Barchi, Jr., for technical assistance on NMR, and Dr. Bob W. Hartley for the expression system of barnase. J.T. is supported by the Japanese Society for the Promotion of Science.

1. Matouschek, A., Kellis, J. T., Jr., Serrano, L., Bycroft, M. & Fersht, A. R. (1990) *Nature (London)* **346,** 440–445.
2. Oliveberg, M. & Fersht, A. R. (1996) *Biochemistry* **35,** 2738–2749.
3. Bycroft, M., Matouschek, A., Kellis, J. T., Jr., Serrano, L. & Fersht, A. R. (1990) *Nature (London)* **346,** 488–491.
4. Sosnick, T. S., Shtilerman, M. D., Mayne, L. & Englander, S. W. (1997) *Proc. Natl. Acad. Sci. USA* **94,** 8545–8550.
5. Qi, P. X., Sosnick, T. R. & Englander, S. W. (1998) *Nat. Struct. Biol.* **5,** 882–887.
6. Jonsson, T., Waldburger, C. D. & Sauer, R. T. (1996) *Biochemistry* **35,** 4795–4802.
7. Otzen, D. E., Kristensen, O., Proctor, M. & Oliverberg, M. (1999) *Biochemistry* **38,** 6499–6511.
8. Chu, R. A., Takei, J., Barchi, J. J., Jr., & Bai, Y. (1999) *Biochemistry* **38,** 14120–14125.
9. Clarke, J. & Fersht, A. R. (1996) *Folding Des.* **1,** 243–254.
10. Yi, Q., Scalley, M. L., Simons, K. T., Gladwin, S. T. & Baker, D. (1997) *Folding Des.* **2,** 271–280.
11. Itzhaki, L. S., Neira, J. L. & Fersht, A. R. (1997) *J. Mol. Biol.* **270,** 89–98.
12. Matouschek, A., Serrano, L. & Fersht, A. R. (1992) *J. Mol. Biol.* **224,** 819–824.
13. Bai, Y., Sosnick, T. R., Mayne, L. & Englander, S. W. (1995) *Science* **269,** 192–197.
14. Schmid, F. X. & Baldwin, R. L. (1979) *J. Mol. Biol.* **135,** 199–205.
15. Bai, Y., Milne, J. S., Mayne, L. & Englander, S. W. (1993) *Proteins* **17,** 75–82.
16. Raschke, T. M. & Marqusee, S. (1997) *Nat. Struct. Biol.* **4,** 298–304.
17. Santoro, M. M. & Bolen, D. W. (1992) *Biochemistry* **31,** 4901–4907.
18. Perrett, S., Clarke, J., Hounslow, A. M. & Fersht, A. R. (1995) *Biochemistry* **34,** 9288–9298.
19. Englander, S. W. & Kallenbach, N. R. (1984) *Q. Rev. Biophys.* **4,** 521–655.
20. Pace, N. C., Laurents, D. V. & Erickson, R. E. (1992) *Biochemistry* **31,** 2728–2734.
21. Jones, D. N., Bycroft, M., Lubinski, M. J. & Fersht, A. R. (1993) *FEBS Lett.* **331,** 165–170.
22. Bai, Y. (1999) *J. Biomol. NMR* **15,** 65–67.
23. Matouschek, A., Matthews, J. M., Johnson, C. M. & Fersht, A. R. (1994) *Protein Eng.* **7,** 1089–1095.
24. Dalby, P. A., Oliveberg, M. & Fersht, A. R. (1998) *J. Mol. Biol.* **276,** 625–646.
25. Matouschek, A. & Fersht, A. R. (1993) *Proc. Natl. Acad. Sci. USA* **90,** 7814–7820.
26. Matthews, J. M. & Fersht, A. R. (1995) *Biochemistry* **34,** 6805–6810.
27. Parker, M. J. & Marqusee, S (1999) *J. Mol. Biol.* **293,** 1195–1210.
28. Clarke, J., Itzhaki, L. S. & Fersht, A. R. (1998) *Trends Biochem. Sci.* **23,** 378–381.
29. Baldwin, R. L. & Rose, G. D. (1999) *Trends Biochem. Sci.* **24,** 24–26.